NUCLEAR INSTRUMENTS AND METHODS 152 (1978) 423-430 ; © NORTH-HOLLAND PUBLISHING CO.

DETECTION OF INDUCED PULSES IN PROPORTIONAL WIRE DEVICES WITH RESISTIVE CATHODES

G. BATTISTONI E. IAROCCI, G. NICOLETTI and L. TRASATTI

Laboratori Nazionali dell'INFN, Frascati, Italy

Received 31 October 1977

If the cathode of a proportional wire device is made out of a suitably resistive material, it is possible to detect induced pulses using pick-up electrodes outside the device itself. Tests have been made on proportional tubes with helical delay lines, strips, or plates as pick-up electrodes. This method simplifies design and construction of pick-up electrodes, and furthermore allows unusual electrode arrangements.

1. Introduction

A widely used method to localize an avalanche along a sense wire in proportional wire devices, is the detection of the pulse induced on suitably shaped cathode electrodes, such as diagonal strips or delay lines. The requirement for an electrode to be both cathode and detection element may create problems and limitations in the design. Remarkable advantages can be gained if the cathode is made out of a continuous resistive layer. In a suitably high range of resistivity the cathode turns out to be transparent to pulsed fields, so that pulses may be detected by any kind of pick-up electrode placed outside the resistive cathode module.

This new type of proportional detector was developed during the study of photon detectors for use with e^+e^- storage ring experiments, in which lengths of up to three meters were required. Preliminary results were given by two of us and other authors in ref. 1. As pick-up electrodes we have used either helical delay lines of the type introduced in ref. 2, or electrodes such as strips or plates.

An interesting result for helix tubes with resistive cathode is that the propagation time may be as high as 20 ns/cm, with an attenuation of ≈ 6 over a 3 m length. Such a long characteristic time permits the use of relatively simple and economical time-to-digital converters. Furthermore it is possible to wind a single helix around an assembly of several tubes, which allows independent optimization in the arrangement of sense wires and helices.

Similarly a single pick-up electrode may be used with resistive tube modules, in many cases simplifying the construction. With this method even unusually complex electrode topologies, such as multicoordinate readout, are possible.

In section 2 we will discuss the principle of operation of the resistive cathode device in the case of tubes with helical delay line readout. In section 3 the helical line behaviour will be described. The results of tests on different kinds of tubes and pick-up electrodes will be reported in sections 4 and 5.

2. The resistive cathode

The principle of operation of a proportional wire device with a resistive cathode will now be discussed, in the case of tubes with helical delay line readout.

A cross-sectional view of such a tube is shown in fig. 1. The anode wire is on the axis of a tube

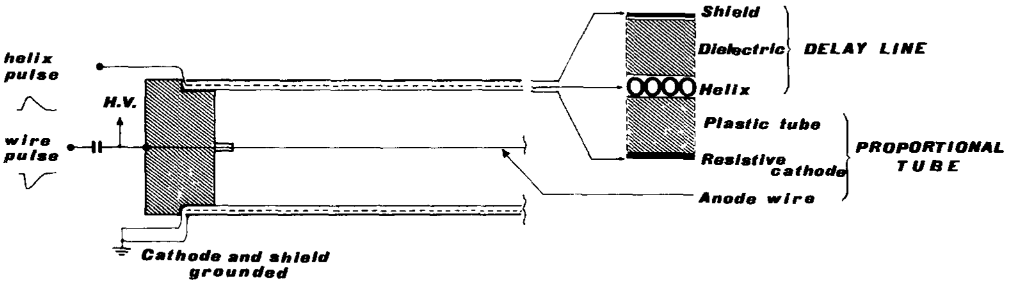

Fig. 1. Longitudinal cross-section of a proportional tube with resistive cathode and external helical delay line.

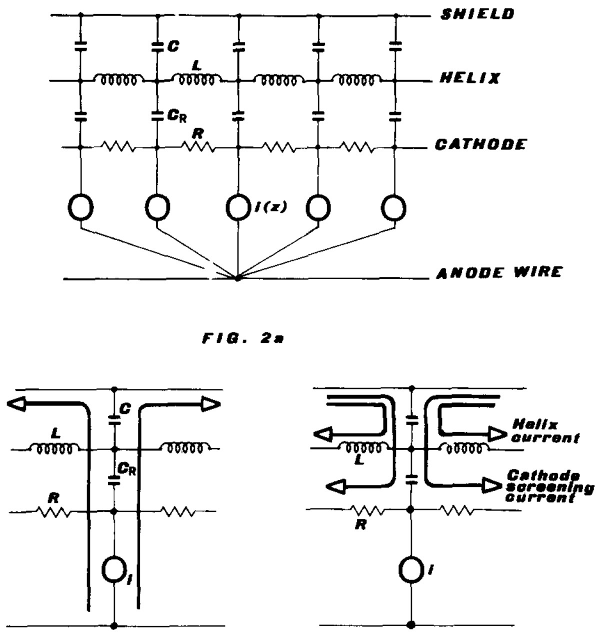

FIG. 2b FIG. 2c

Fig. 2. Equivalent circuit for a resistive cathode tube with helical delay-line readout.

made of polyvinylchloride (PVC), having an internal resistive coating. The delay line consists of a helix of conductive wire wound around the tube, followed by an insulating gap (the dielectric medium of the delay line), and a conductive foil (its ground electrode).

The equivalent circuit describing the operation of the tube is shown in fig. 2a. The current generators $i(z)$ simulate the proportional counter signal, z being along the tube axis. $i(z)$ has a bell shaped distribution around the avalanche point with a width of the order of the tube diameter. R is the specific resistance of the cathode and C_R its specific capacitance to the helix, while L and C are the specific inductance and capacitance of the delay line. These specific values are given per unit tube length.

At the beginning of the induction process, we will assume that current from each generator flows into the lowest impedance loop, charging the capacitance C_c given by the series capacitance of C_R and C (fig. 2b). Now C can (fig. 2c) either discharge into the neighbouring elements of the LC line (pulse transmission) or in the neighbouring elements of the RC_c line (screening effect of the cathode). In this schematic picture the resistive cathode is transparent to the induced signal if C is discharged faster by the LC line than C_c by the RC_c one.

The order of magnitude of the minimum cathode specific resistance can be estimated as follows. Since the width along z of the induced current distribution is of the order of the tube diameter D, the transmission time over such a length, τD, must be compared with the basic time constant associated to the RC_c line, RC_cD^2. From these considerations the following transparency condition is obtained:

$$R \gtrsim \tau/(C_c D). \qquad (1)$$

Since in practice $C_c \approx C$, eq. (1) can be written as follows:

$$R \gtrsim Z_0/D, \qquad (2)$$

where Z_0 is the characteristic impedance of the delay line.

Taking into account a reasonable range of the parameters, the minimum value for R turns out to be 10^2–10^3 Ω/cm.

Furthermore, the value of R should be large enough to have no effect on the delay line characteristics. The resistive cathode introduces a distributed impedance in parallel with the helix inductance, given by the series combination C_R-R-C_R. This impedance must be much larger than the impedance of the inductance over the frequency spectrum of the transmitted pulse. This is equivalent to require

$$L/R \ll t_r, \qquad (3)$$

where t_r can be taken as the pulse rise time. Here we have assumed conservatively that C_c is very large. Eq. (3) may be written as follows:

$$R \gg \tau Z_0/t_r. \qquad (4)$$

For propagation times of less than a few ns/cm, which can be associated with low characteristic impedance values ($Z_0 \approx 10^2$ Ω) the minimum value for R is about 10^3 Ω/cm (see section 4). For τ as high as 20 ns/cm which require high values of Z_0 to maintain a tolerable distortion, the limit for R increases to 10^5 Ω/cm.

Even in this extreme case the limit in the counting rate set by the tube resistance is largely below the limit set by the long memory time given by the high τ.

The resistive coating can be realized with different kinds of varnishes. For low resistivity values ($< 5 \times 10^4$ Ω/square) we have used commercial colloidal graphite in water or 2-propanol. The resistivity range may be extended up to

$\approx 10^7$ Ω/square using a mixture of graphite or carbon black with a polyacetovinylic emulsion.

3. Helical delay line

Preliminary observations on helical delay lines showed two important qualitative effects:

1) the shield must be highly and continuously conductive over its whole circular cross-section, otherwise the transmission properties of the line are strongly impaired for large delays;
2) when conditions 1) is satisfied, the delay for a given compact-wound helix depends essentially on the relative dielectric constant ε_r of the insulating layer between helix and shield.

The first observation suggests that the return current on the continuous shield flows helically, following with opposite sense of rotation the current in the helix, thus confining the electromagnetic field to the gap between helix and shield. Under this hypothesis and approximating the current in the compact helix by a cylindrical current sheet, the inductance L per unit axial length of the delay line is given by:

$$L = L_s - L_h, \tag{5}$$

where L_h and L_s are the inductance per unit axial length of two cylindrical current sheets with the same winding density, the diameters of which equal those of the helix and the shield respectively.

Eq. (5) may be expressed as follows:

$$L = 0.004\pi^2 \frac{(D+d)\,d}{p^2}\ \mu\text{H/cm}, \tag{6}$$

where D is the helix diameter, d the distance between helix and shield, and p the helix pitch.

Again approximating the helix with a continuous cylindrical conductor, and assuming $d \ll D$, the associated specific capacitance is given by:

$$C = 0.0885\varepsilon_r \frac{\pi(D+d)}{d}\ \text{pF/cm}. \tag{7}$$

From these expressions for L and C we can calculate the delay line characteristic impedance and propagation time:

$$Z_0 = \sqrt{\left(\frac{L}{C}\right)} = 377 \frac{1}{\sqrt{\varepsilon_r}} \frac{d}{p}\,\Omega, \tag{8}$$

$$\tau = \sqrt{(LC)} = \frac{\sqrt{\varepsilon_r}}{c} \frac{\pi(D+d)}{p}\ \text{ns/cm}. \tag{9}$$

c is the speed of light in vacuum. Noticing in eq. (9) that the term $\pi(D+d)/p$ is simply the helical delay line length l_h per unit tube lenght, this equation may also be written:

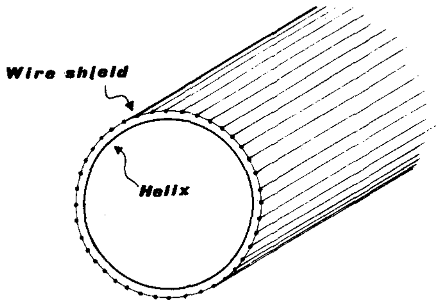

Fig. 3. Schematic diagram of a helix tube with the ground electrode made out of longitudinal wires.

$$\tau = \frac{\sqrt{\varepsilon_r}}{c}\, l_h. \tag{10}$$

This expression is identical to that for a coaxial line. The τ and Z_0 values computed using eqs. (8) and (9) are in good agreement with the experimental values, within the given approximations.

The statement that the shield must be a continuous cylinder in order to achieve a distortionless transmission, and the inductance expression (6) as a function of the geometrical parameters, are in disagreement with what found by G. Flügge et al.[2]). They suggest as an important construction detail to use a cylindrical shield with a longitudinal slit. In this way the helical flow of the return current in the shield is inhibited, and in fact in their expression for the specific inductance no dependence appears on the helix–shield distance. This is equivalent to assume zero mutual induction between helix and shield. This would seem not to be true, and in practice several undesirable effects take place with a discontinuous shield, which are tolerable only for small total delays, like those in ref. 2. We have made a test in an extreme case where the ground electrode was made out of longitudinal wires (see fig. 3), in order to minimize the helical conduction. The response of this line ($D = 3$ cm, $d = 1$ mm, $p = 1$ mm) to a step voltage pulse is shown in fig. 4. A ringing waveform starts at time t_1, with increasing amplitude and decreasing frequency, until the voltage damps down to the asymptotic level at time t_2. The remarkable fact is that the delay t_1, corresponds to that of the same helix and dielectric assembly with a continuous cylindrical shield (full mutual induction), while t_2 is the delay expected for the case of no mutual inductance.

We can explain this behaviour in the following

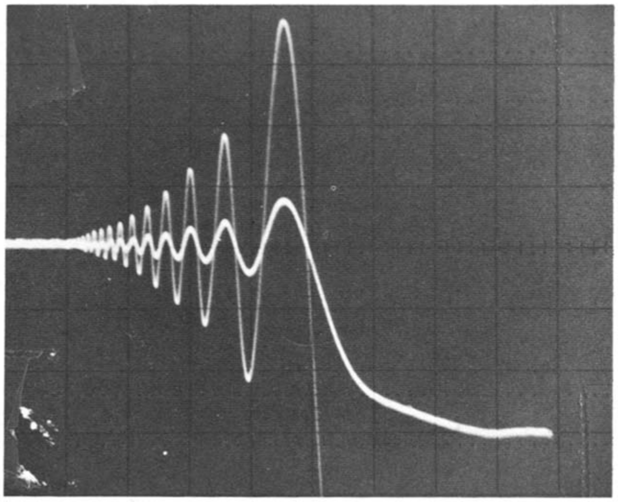

Fig. 4. Response of the line of fig. 3 to a negative step voltage. The same picture is repeated with two different vertical scales to show the details of the ringing waveform, abscissa 200 ns/div.

way. There is a distributed capacitive coupling between the wires of the ground electrode (see fig. 3), which allows the helical conduction and thus introduces a mutual inductance. This mutual inductance however is now a function of frequency, being a maximum at high frequency and zero at low frequency, inferring that the propagation time itself is a function of frequency. As a consequence the high frequency components of the step voltage are spread out in time during the transmission and interfere with each other giving rise to the observed ringing waveform. This interpretation is confirmed by the fact that increasing the step voltage risetime, the oscillation is gradually cancelled out. This effect is clearly unavoidable since for any discontinuous shield there will always be a capacitance acting as a short circuit for the high frequency components.

4. Tests on resistive tubes with helical delay line readout

We will now describe the operation of tubes with helical readout for two different values of the characteristic propagation time of the helical delay line: 3 ns/cm (fast helix) and 20 ns/cm (slow helix). Then the possibility of multiple tube readout by a single helix will be discussed.

4.1. Fast helix

The proportional tube is made out of a 1 m long PVC tube (17 mm inner, 19 mm outer diameter), with a 40 μm or 100 μm sense wire, and on the inside surface a 2 kΩ/cm resistive cathode coating. The helical line is made by a compact winding of 5 helices (160 μm double enamelled Cu wire) connected in parallel at both ends, thereby simulating a helical strip of 1 mm pitch. The dielectric medium is one layer of a 0.15 mm thick teflon foil attached by scotch tape. The covering shield is a 50 μm thick aluminum foil.

The measured parameters of this line are the following:

$\tau = 3.0$ ns/cm, $\quad Z_0 = 92\,\Omega$.

formulas (8) and (9) give only approximate predictions for this extreme geometry (very thin dielectric):

$\tau = 2.86$ ns/cm, $\quad Z_0 = 76\,\Omega$.

Fig. 6 shows the pulses generated by an uncollimated β source placed at a distance of 5 cm from one end of the tube, as detected: a) on the wire (50 Ω load), b) on the helix end (100 Ω load) near the source, c) on the helix end far from the source. The sense wire diameter is 40 μm, and the gas mixture 70% argon + 30% isobutane: the tube is operated in the limited Geiger mode (see next section). Comparison of helix pulse height near the source with wire pulse height shows the full transparency to induction of the resistive cathode. The attenuation of the helix pulse after 1 m transmission distance is a factor of 2 and is essentially due to the resistance of the helix wire.

In order to study the influence of the cathode resistivity on the delay propagation parameters we

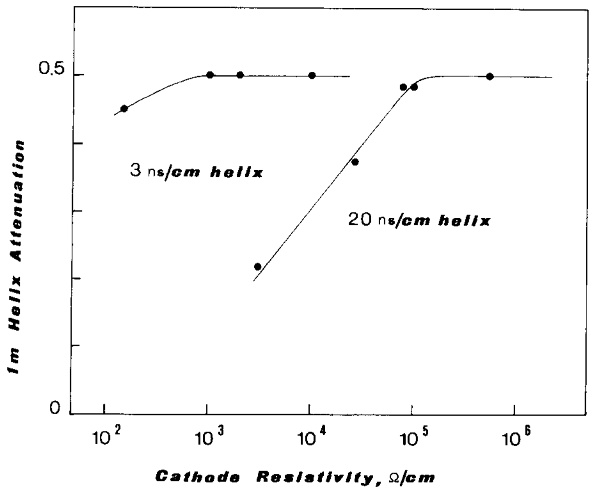

Fig. 5. Attenuation vs cathode resistivity for two different helical delay line tubes for a triangular pulse (30 ns risetime, 300 ns duration).

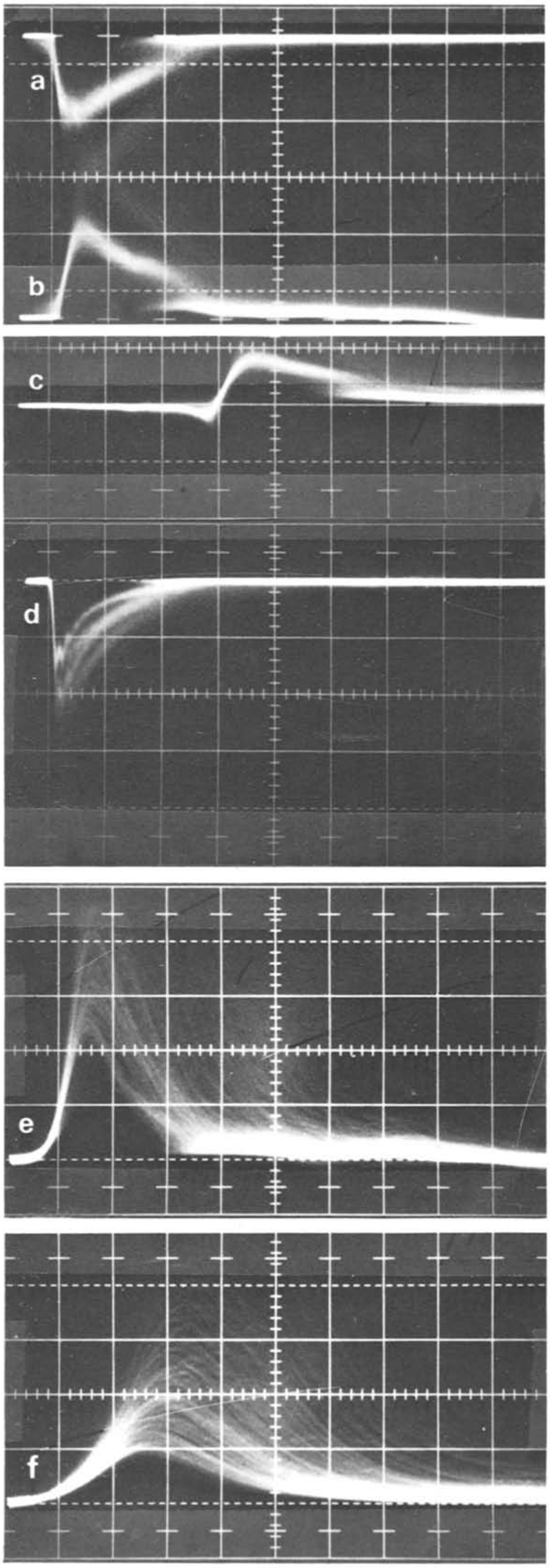

measured the attenuation of a standard pulse (triangular 30 ns rise time, 300 ns duration), on the 1 m long line varying the cathode resistivity (see fig. 5). No effect was observed for $R \geqslant 1\ \mathrm{k}\Omega/\mathrm{cm}$. Even when the cathode resistivity was as low as $150\ \Omega/\mathrm{cm}$ the attenuation was increased only by 10%.

4.2. Slow helix

4.2.1. *Tube geometry*

The test tube is a PVC tube (30.0 mm inner and 32.5 mm outer diameter), with a $100\ \mathrm{k}\Omega/\mathrm{cm}$ cathode on the inside and a $100\ \mu\mathrm{m}$ anode wire.

The helix is a compact winding of 0.2 mm double enamelled copper wire, the resulting pitch being 0.25 mm. The dielectric medium (1.2 mm thickness) is made out of a rolled plastic foil ($\varepsilon_r = 2$). The shield is a $30\ \mu\mathrm{m}$ thick Cu foil. The measured parameters of this delay line are:

$\tau = 20\ \mathrm{ns/cm}$, $Z_0 = 1.4\ \mathrm{k}\Omega$,

in agreement with the values predicted by eqs. (8) and (9):

$\tau = 19.6\ \mathrm{ns/cm}$, $Z_0 = 1.42\ \mathrm{k}\Omega$, respectively

4.2.2. *Wire signals*

Sence wires $\gtrsim 50\ \mu\mathrm{m}$ in diameter make it possible to operate the tube in the limited Geiger mode[3]). The advantage of working in this regime is that the minimum pulse height generated on the wire is $\approx 40\ \mathrm{mV}/50\ \Omega$. This allows the use of relatively high thresholds even for long helices. The long local dead time characteristic of this regime ($330\ \mu\mathrm{s}$ for the ≈ 1 cm long Geiger region) is compatible with the maximum statistical rate tolerable due to the long memory of the slow helix ($2\ \mu\mathrm{s/m}$). Fig. 6d shows the pulses generated by an uncollimated β source as detected on the wire. The load resistance is $50\ \Omega$, the gas mixture is argon+ethane (40/60), the anode voltage 4.1 kV.

Typical curves of singles rate and average current vs high voltage for a 1 m long tube are shown in fig. 7 for argon–isobutane or argon-ethane gas

Fig. 6. Pulse shapes from a ^{90}Sr beta source for two different tubes. Fast helix (argon–isobutane (70/30), HV = 3.3 kV, 17 mm diameter tube, $40\ \mu\mathrm{m}$ diameter sense wire): a) wire pulse ($50\ \Omega$ load); b) helix pulse 5 cm far from the source ($100\ \Omega$ load); c) helix pulse 95 cm far from the source ($100\ \Omega$ load). Slow helix (argon–ethane (40/60), HV = 4.1 kV 30 mm diameter tube, $100\ \mu\mathrm{m}$ diameter sense wire); d) wire pulse ($50\ \Omega$ load); e) helix pulse 5 cm far from the source ($50\ \Omega$ load); f) helix pulse 250 cm far from the source ($50\ \Omega$ load); abscissa a)–f): 100 ns/div., coordinate a), b), c) and e): 20 mV/div., d): 50 mV/div. and f): 10 mV/div.

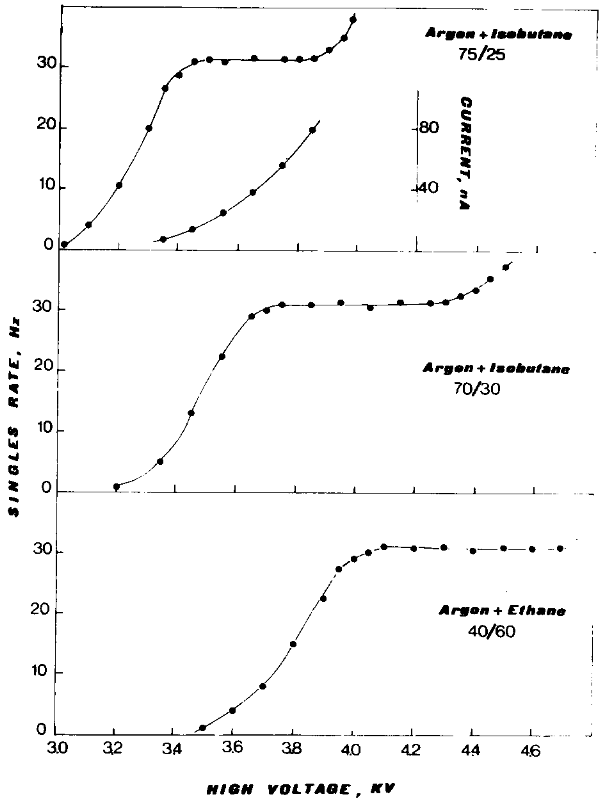

Fig. 7. Singles rate and average current vs HV for different gas mixtures (30 mm tube diameter, 100 μm sense wire diameter).

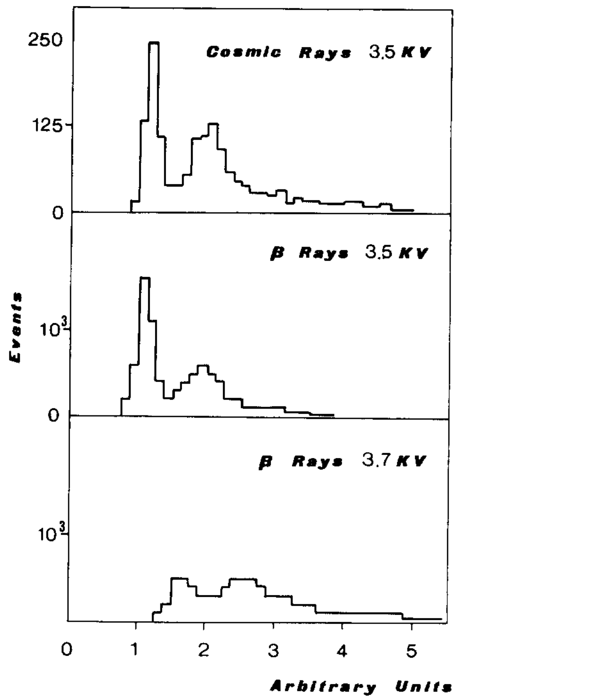

Fig. 8. Wire pulse height spectra for cosmic rays and beta rays (30 mm tube diameter, 100 μm sense wire diameter, argon–isobutane 75/25).

mixtures. The signals are shaped to 0.5 μs duration and the threshold is 30 mV on a 50 Ω load. There is a wide plateau where only particles are counted. This plateau coincides with the efficiency plateau as measured on a layer of tubes. The inefficiency region near the wall is estimated to be <1 mm.

The wire pulse height spectrum for cosmic rays at 3.5 kV (Ar+isobutane, 75/25) is shown in fig. 8a. It has been obtained by integrating the wire pulse around the maximum by an 8 ns gate. The spectrum shows two clear peaks and if the gate is lengthened the number of such peaks increases. An identical spectrum is obtained with an uncollimated ^{90}Sr source (see fig. 8b). On the other hand if the source is collimated, the second peak is strongly depressed. This fact suggests that the multiple peak structure of the spectrum is due to multiple limited Geiger processes triggered by tracks at an angle with the wire such that their projection on it is larger than the first Geiger region. In fact in this case electrons will reach the wire outside the region of the first Geiger discharge and can trigger one or more new ones.

4.2.3. *Helix signal*

Figs 6e and 6f show the helix signals associated to the wire signals of fig. 6d, at a propagation distance of 5 and 250 cm respectively: this was possible by connecting three identical 1 m long tubes in series. The attenuation of the transmitted signal after 2.5 m is a factor of 5. The pulse risetime is 160 ns. Such distorsion of the pulse is not influenced by the resistive cathode (100 kΩ/cm) as can be seen in fig. 5 where the attenuation of a 1 m long 20 ns/cm helix is plotted as a function of cathode resistivity.

The spatial resolution of the helix readout is essentially limited by the following two effects:

a) a systematic non linearity due to the increase of the risetime with distance,
b) a spread in the position measurement due to the amplitude jitter.

The spectrum in fig. 9 gives a measure of the spread in the position measurement due to the amplitude jitter: un uncollimated β source was placed in the middle of a 3 m long helix (3 tubes in series), and the sum of the two delays measured at the ends of the helix with respect to the wire pulse was recorded. By this way the spread in the source width is cancelled out, and what is left

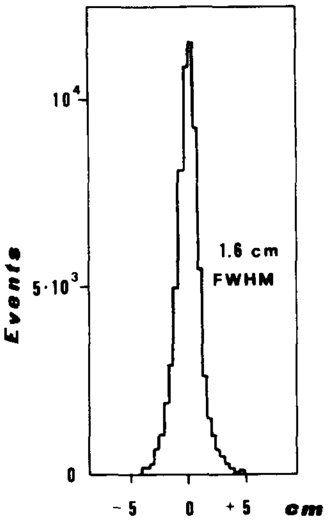

Fig. 9. Spread in the position measurement on a 20 ns/cm helical delay line read at 1.5 m distance from the source, compensated for source spread (30 mm tube diameter, 100 μm wire diameter, HV = 3.8 kV, argon–isobutane 75/25).

is twice the spread of the single readout after 1.5 m transmission distance, which turns out to be 16 mm fwhm. This is the worst case for a 3 m long tube if helix pulse delay with respect to the wire pulse is measured at both ends. Furthermore since the total delay of a helix delay line can be considered a known and stable quantity, double readout allows to correct in first approximation the effects of rise time and amplitude jitter, a) and b).

4.3. Multiple tube assembly

An interesting possibility is that more than one resistive cathode tube can be assembled together enclosed in a single helical winding, so OR-ing together the induced pulses from each tube on the same helix. We have tested this possibility by assembling together in a triangle 3 tubes (1 m long, 3 cm diameter, $R = 100$ kΩ/cm) and winding around them a single helix (0.3 mm Cu wire diameter, 0.4 mm helix pitch), followed by a rolled plastic foil dielectric (1 mm thickness, $\varepsilon_r = 2$) and a copper shield. The characteristic propagation time was 25 ns/cm. No undesired effect was observed, in particular the signal induced from one wire on the two neighbours was negligible.

Such multitube arrangement allows independent optimization of the pattern of wires and helices. Furthermore extruded multitube plastic modules are industrially produced for many practical applications, so that it is possible to obtain specially designed cross-section geometries.

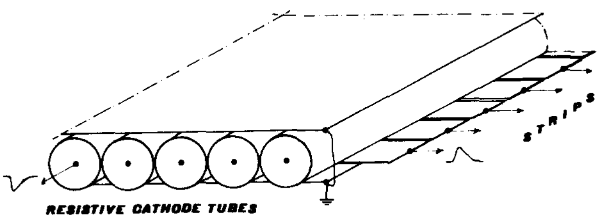

Fig. 10. Resistive tubes with strips as pick-up electrodes.

5. Tests on resistive tube modules with external pick-up electrodes

We have made some qualitative tests concerning the detection of induced pulses by strip or plate electrodes, placed outside a layer of resistive cathode tubes. The test module is shown in fig. 10. The pick-up electrode is made out of a foil of double clad printed circuit board ($0.1 \times 50 \times 100$ cm^3). On one side the copper layer is cut into 2 cm wide strips with a 200 pF capacitance to ground. The foil is placed on one side of a set of tubes 2 cm in diameter, 0.5 m long, with the strips facing the tubes orthogonally to the wires. Another copper foil is placed on the other side of the tubes, and is grounded together with that on the back of the strips. The tubes have 100 μm sense wires and are operated in the limited Geiger mode.

Similarly to the case of the helix readout there is a useful range of the cathode resistivity allowing induced pulse detection without limiting tube operation at high rates. Once a useful signal is picked up on the strips near the induction region (transparency condition), there are two conditions which must be satisfied:

a) the local voltage drop on the resistive cathode due to the screening current must not capacitively induce appreciable pulses on strips far from the avalanche;
b) the cross-talk between strips due to RC coupling via all the cathodes must be negligible.

The scheme of the system in fig. 11 illustrates the situation.

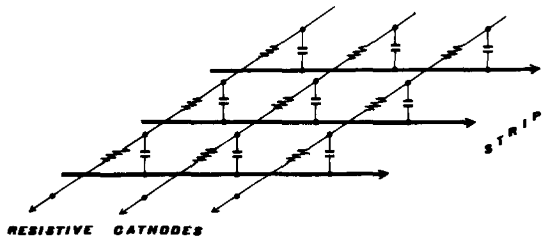

Fig. 11. Equivalent circuit for the test set up of fig. 10.

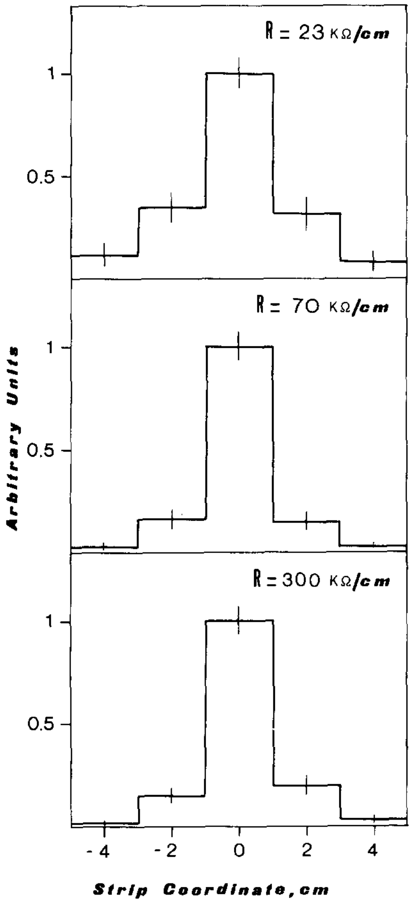

Fig. 12. Pulse height on different strips from a collimated ^{55}Fe X-ray source for different values of cathode resistivity.

We have experimentally verified that in this geometry effect b) is negligible with respect to effect a) for strip lengths up to a few meters. Tests were made using resistive foils to simulate multitube layers.

Effect a) was studied measuring the pulse height distribution over the strips with a collimated ^{55}Fe source placed on a tube at the center of a strip. Three different values of cathode resistivity were used, and the resulting amplitude distributions over the strips are shown in fig. 12. The strips were loaded on 50 Ω and the pulse height on the central strip was $\approx 1/3$ of that on the wire with the same load resistance. From such distributions we conclude that for cathode resistivities larger than ≈ 50 kΩ/cm, with the given geometrical parameters, the effect is negligible.

By this method it is very easy to construct pick-up electrodes even in rather untrivial topologies. We have made a qualitative test of the two following electrode arrays:

1) a bidimensional array (50×60 cm^2) of rectangular electrodes (10×12 cm^2),
2) a "chessboard" array of plate electrodes where the "white" squares are connected along one of the diagonals and the "black" squares along the other one, allowing the measurement of two coordinates on a single pick-up plane.

We wish to thank J. E. Augustin, B. Greland, S. Jullian, B. Jean Marie, G. Parrour and F. Rumpf, for many stimulating discussions and suggestions. We are grateful to G. Mazzenga and A. Rutili who built the test modules.

References

1) V. Bidoli et al., Frascati Report LNF-76/58 (R) (1976).
2) G. Flügge et al., Report DESY F 1/F 33/F 39-76/05 (1976).
3) S. Brehil et al., Nucl. Instr. and Meth. **123** (1975) 225.